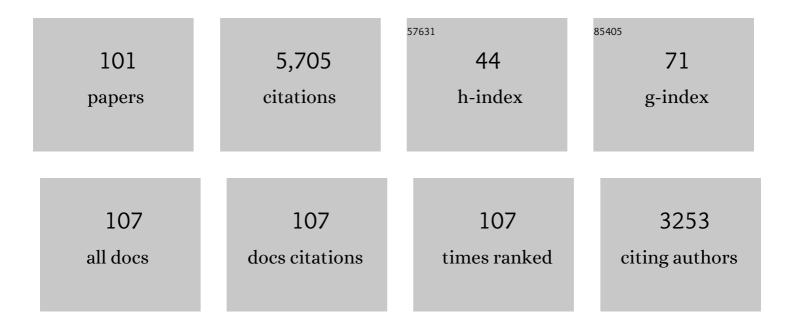
## Xiang-Yu Kong

List of Publications by Year in descending order

Source: https://exaly.com/author-pdf/4538144/publications.pdf Version: 2024-02-01



XIANC-YU KONC

#	Article	IF	CITATIONS
1	Ionic Crosslinkingâ€Induced Nanochannels: Nanophase Separation for Ion Transport Promotion. Advanced Materials, 2022, 34, e2108410.	11.1	25
2	The synergistic effect of space and surface charge on nanoconfined ion transport and nanofluidic energy harvesting. Nano Energy, 2022, 92, 106709.	8.2	14
3	Bioinspired hierarchical porous membrane for efficient uranium extraction from seawater. Nature Sustainability, 2022, 5, 71-80.	11.5	112
4	Electrochemical ion-pumping-assisted transfer system featuring a heterogeneous membrane for lithium recovery. Chemical Engineering Journal, 2022, 435, 134955.	6.6	12
5	Polymer-based membranes for promoting osmotic energy conversion. Giant, 2022, 10, 100094.	2.5	21
6	Covalent organic frameworks embedded in polystyrene membranes for ion sieving. Chemical Communications, 2022, 58, 5403-5406.	2.2	12
7	Engineered Cellulose Nanofiber Membranes with Ultrathin Low-Dimensional Carbon Material Layers for Photothermal-Enhanced Osmotic Energy Conversion. ACS Applied Materials & Interfaces, 2022, 14, 13223-13230.	4.0	31
8	Biomimetic KcsA channels with ultra-selective K+ transport for monovalent ion sieving. Nature Communications, 2022, 13, 1701.	5.8	46
9	Bioinspired poly (ionic liquid) membrane for efficient salinity gradient energy harvesting: Electrostatic crosslinking induced hierarchical nanoporous network. Nano Energy, 2022, 97, 107170.	8.2	18
10	Wetting-Induced Water Promoted Flow on Tunable Liquid–Liquid Interface-Based Nanopore Membrane System. ACS Nano, 2022, 16, 11092-11101.	7.3	7
11	Anion Concentration Gradient-Assisted Construction of a Solid–Electrolyte Interphase for a Stable Zinc Metal Anode at High Rates. Journal of the American Chemical Society, 2022, 144, 11168-11177.	6.6	94
12	Cement-and-pebble nanofluidic membranes with stable acid resistance as osmotic energy generators. Science China Materials, 2022, 65, 2729-2736.	3.5	2
13	Tailoring Sulfonated Poly(phenyl-alkane)s of Intrinsic Microporosity Membrane for Advanced Osmotic Energy Conversion. , 2022, 4, 1422-1429.		11
14	lon transport regulation through triblock copolymer/PET asymmetric nanochannel membrane: Model system establishment and rectification mapping. Chinese Chemical Letters, 2021, 32, 822-825.	4.8	29
15	Charged porous asymmetric membrane for enhancing salinity gradient energy conversion. Nano Energy, 2021, 79, 105509.	8.2	42
16	A universal functionalization strategy for biomimetic nanochannel via external electric field assisted non-covalent interaction. Nano Research, 2021, 14, 1421-1428.	5.8	16
17	Metal organic framework enhanced SPEEK/SPSF heterogeneous membrane for ion transport and energy conversion. Nano Energy, 2021, 81, 105657.	8.2	47
18	Metallic Two-Dimensional MoS <sub>2</sub> Composites as High-Performance Osmotic Energy Conversion Membranes. Journal of the American Chemical Society, 2021, 143, 1932-1940.	6.6	133

#	Article	IF	CITATIONS
19	Nacre-like Mechanically Robust Heterojunction for Lithium-Ion Extraction. Matter, 2021, 4, 737-754.	5.0	69
20	An Efficient Uranium Adsorption Magnetic Platform Based on Amidoxime-Functionalized Flower-like Fe <sub>3</sub> O <sub>4</sub> @TiO <sub>2</sub> Core–Shell Microspheres. ACS Applied Materials & Interfaces, 2021, 13, 17931-17939.	4.0	104
21	Light-Induced Heat Driving Active Ion Transport Based on 2D MXene Nanofluids for Enhancing Osmotic Energy Conversion. CCS Chemistry, 2021, 3, 1325-1335.	4.6	48
22	A joint experimental and theoretical study on structural, electronic, and magnetic properties of MnGenâ^' (n = 3–14) clusters. Journal of Chemical Physics, 2021, 154, 204302.	1.2	24
23	Surface Charge Regulated Asymmetric Ion Transport in Nanoconfined Space. Small, 2021, 17, e2101099.	5.2	31
24	Thermoenhanced osmotic power generator via lithium bromide and asymmetric sulfonated poly(ether) Tj ETQq0	0 9 ggBT /	Overlock 10 1
25	Heterogeneous MXene/PSâ€bâ€P2VP Nanofluidic Membranes with Controllable Ion Transport for Osmotic Energy Conversion. Advanced Functional Materials, 2021, 31, 2105013.	7.8	62
26	Biomimetic Nanocomposite Membranes with Ultrahigh Ion Selectivity for Osmotic Power Conversion. ACS Central Science, 2021, 7, 1486-1492.	5.3	48
27	Synergy of light and acid–base reaction in energy conversion based on cellulose nanofiber intercalated titanium carbide composite nanofluidics. Energy and Environmental Science, 2021, 14, 4400-4409.	15.6	53
28	Tunable molecular transport and sieving enabled by covalent organic framework with programmable surface charge. Materials Today, 2021, 51, 56-64.	8.3	19
29	Ultrathin and Robust Silk Fibroin Membrane for High-Performance Osmotic Energy Conversion. ACS Energy Letters, 2020, 5, 742-748.	8.8	98
30	Specific Recognition of Uranyl Ion Employing a Functionalized Nanochannel Platform for Dealing with Radioactive Contamination. ACS Applied Materials & Interfaces, 2020, 12, 3854-3861.	4.0	24
31	Improved Ion Transport in Hydrogel-Based Nanofluidics for Osmotic Energy Conversion. ACS Central Science, 2020, 6, 2097-2104.	5.3	49
32	Underwater superaerophobic Ni nanoparticle-decorated nickel–molybdenum nitride nanowire arrays for hydrogen evolution in neutral media. Nano Energy, 2020, 78, 105375.	8.2	148
33	Biomimetic Nacre-Like Silk-Crosslinked Membranes for Osmotic Energy Harvesting. ACS Nano, 2020, 14, 9701-9710.	7.3	124
34	Improved Ion Transport and High Energy Conversion through Hydrogel Membrane with 3D Interconnected Nanopores. Nano Letters, 2020, 20, 5705-5713.	4.5	71
35	pH-regulated thermo-driven nanofluidics for nanoconfined mass transport and energy conversion. Nanoscale Advances, 2020, 2, 4070-4076.	2.2	6
36	Enhanced ion transport by graphene oxide/cellulose nanofibers assembled membranes for high-performance osmotic energy harvesting. Materials Horizons, 2020, 7, 2702-2709.	6.4	118

#	Article	IF	CITATIONS
37	Tailoring A Poly(ether sulfone) Bipolar Membrane: Osmoticâ€Energy Generator with High Power Density. Angewandte Chemie - International Edition, 2020, 59, 17423-17428.	7.2	47
38	Bioinspired hydrogel-based nanofluidic ionic diodes: nano-confined network tuning and ion transport regulation. Chemical Communications, 2020, 56, 8123-8126.	2.2	16
39	Neutralization Reaction Assisted Chemical-Potential-Driven Ion Transport through Layered Titanium Carbides Membrane for Energy Harvesting. Nano Letters, 2020, 20, 3593-3601.	4.5	76
40	Tailoring A Poly(ether sulfone) Bipolar Membrane: Osmoticâ€Energy Generator with High Power Density. Angewandte Chemie, 2020, 132, 17576-17581.	1.6	11
41	Bioinspired nervous signal transmission system based on two-dimensional laminar nanofluidics: From electronics to ionics. Proceedings of the National Academy of Sciences of the United States of America, 2020, 117, 16743-16748.	3.3	22
42	Towards Practical Osmotic Energy Capture by a Layer-by-Layer Membrane. Trends in Chemistry, 2020, 2, 180-182.	4.4	16
43	Robust sulfonated poly (ether ether ketone) nanochannels for high-performance osmotic energy conversion. National Science Review, 2020, 7, 1349-1359.	4.6	65
44	High-performance silk-based hybrid membranes employed for osmotic energy conversion. Nature Communications, 2019, 10, 3876.	5.8	252
45	Engineered PES/SPES nanochannel membrane for salinity gradient power generation. Nano Energy, 2019, 59, 354-362.	8.2	71
46	Engineered Smart Gating Nanochannels for High Performance in Formaldehyde Detection and Removal. Advanced Functional Materials, 2019, 29, 1807953.	7.8	53
47	A photoelectron spectroscopy and quantum chemical study on ternary Al–B–O clusters: Al <sub>n</sub> BO <sub>2</sub> <sup>â^'</sup> and Al <sub>n</sub> BO <sub>2</sub> ( <i>n</i> = 2, 3). Physical Chemistry Chemical Physics, 2018, 20, 5200-5209.	1.3	1
48	Bioinspired Heterogeneous Ion Pump Membranes: Unidirectional Selective Pumping and Controllable Gating Properties Stemming from Asymmetric Ionic Group Distribution. Journal of the American Chemical Society, 2018, 140, 1083-1090.	6.6	87
49	Light- and Electric-Field-Controlled Wetting Behavior in Nanochannels for Regulating Nanoconfined Mass Transport. Journal of the American Chemical Society, 2018, 140, 4552-4559.	6.6	99
50	A bio-inspired dumbbell-shaped nanochannel with a controllable structure and ionic rectification. Nanoscale, 2018, 10, 6850-6854.	2.8	25
51	Biomimetic Peptideâ€Gated Nanoporous Membrane for Onâ€Demand Molecule Transport. Angewandte Chemie, 2018, 130, 157-161.	1.6	12
52	Biomimetic Peptideâ€Gated Nanoporous Membrane for Onâ€Demand Molecule Transport. Angewandte Chemie - International Edition, 2018, 57, 151-155.	7.2	41
53	Bacteriorhodopsinâ€Inspired Lightâ€Driven Artificial Molecule Motors for Transmembrane Mass Transportation. Angewandte Chemie, 2018, 130, 16950-16954.	1.6	6
54	Bacteriorhodopsinâ€Inspired Lightâ€Driven Artificial Molecule Motors for Transmembrane Mass Transportation. Angewandte Chemie - International Edition, 2018, 57, 16708-16712.	7.2	40

#	Article	IF	CITATIONS
55	Light-Driven ATP Transmembrane Transport Controlled by DNA Nanomachines. Journal of the American Chemical Society, 2018, 140, 16048-16052.	6.6	76
56	A universal tunable nanofluidic diode via photoresponsive host–guest interactions. NPG Asia Materials, 2018, 10, 849-857.	3.8	30
57	Skinâ€Inspired Lowâ€Grade Heat Energy Harvesting Using Directed Ionic Flow through Conical Nanochannels. Advanced Energy Materials, 2018, 8, 1800459.	10.2	47
58	Bioinspired Ionic Diodes: From Unipolar to Bipolar. Advanced Functional Materials, 2018, 28, 1801079.	7.8	82
59	Structural evolution and magnetic properties of anionic clusters Cr <sub>2</sub> Ge <sub> <i>n</i> </sub> ( <i>n</i> = 3–14): photoelectron spectroscopy and density functional theory compu Journal of Physics Condensed Matter, 2018, 30, 335501.	ut <b>et†</b> on.	20
60	Engineered Artificial Nanochannels for Nitrite Ion Harmless Conversion. ACS Applied Materials & Interfaces, 2018, 10, 30852-30859.	4.0	17
61	High-Sensitivity Detection of Iron(III) by Dopamine-Modified Funnel-Shaped Nanochannels. ACS Applied Materials & Interfaces, 2018, 10, 22632-22639.	4.0	67
62	Sequential Recognition of Zinc and Pyrophosphate Ions in a Terpyridineâ€Functionalized Single Nanochannel. ChemPhysChem, 2017, 18, 253-259.	1.0	15
63	A Tunable Ionic Diode Based on a Biomimetic Structureâ€īailorable Nanochannel. Angewandte Chemie - International Edition, 2017, 56, 8168-8172.	7.2	72
64	A Tunable Ionic Diode Based on a Biomimetic Structure‶ailorable Nanochannel. Angewandte Chemie, 2017, 129, 8280-8284.	1.6	7
65	Ultrathin and Ion-Selective Janus Membranes for High-Performance Osmotic Energy Conversion. Journal of the American Chemical Society, 2017, 139, 8905-8914.	6.6	304
66	An Artificial CO <sub>2</sub> â€Driven Ionic Gate Inspired by Olfactory Sensory Neurons in Mosquitoes. Advanced Materials, 2017, 29, 1603884.	11.1	61
67	Structural and magnetic properties of FeGenâ^'/O (n = 3-12) clusters: Mass-selected anion photoelectron spectroscopy and density functional theory calculations. Journal of Chemical Physics, 2017, 147, 234310.	1.2	32
68	Photoelectron Spectroscopy and Density Functional Calculations of TiGe <i>n</i> â^' ( <i>n</i> =7–12) Clusters. Chinese Journal of Chemical Physics, 2016, 29, 123-128.	0.6	18
69	Highly Conductive, Airâ€6table Silver Nanowire@Iongel Composite Films toward Flexible Transparent Electrodes. Advanced Materials, 2016, 28, 7167-7172.	11.1	203
70	Engineered Asymmetric Composite Membranes with Rectifying Properties. Advanced Materials, 2016, 28, 757-763.	11.1	31
71	Adenosineâ€Activated Nanochannels Inspired by Gâ€Protein oupled Receptors. Small, 2016, 12, 1854-1858.	5.2	26
72	A Biomimetic Voltageâ€Gated Chloride Nanochannel. Advanced Materials, 2016, 28, 3181-3186.	11.1	77

#	Article	IF	CITATIONS
73	Enhanced Stability and Controllability of an Ionic Diode Based on Funnel‧haped Nanochannels with an Extended Critical Region. Advanced Materials, 2016, 28, 3345-3350.	11.1	109
74	Light ontrolled Ion Transport through Biomimetic DNAâ€Based Channels. Angewandte Chemie, 2016, 128, 15866-15870.	1.6	20
75	A Bioinspired Multifunctional Heterogeneous Membrane with Ultrahigh Ionic Rectification and Highly Efficient Selective Ionic Gating. Advanced Materials, 2016, 28, 144-150.	11.1	179
76	Electrostatic-Charge- and Electric-Field-Induced Smart Gating for Water Transportation. ACS Nano, 2016, 10, 9703-9709.	7.3	63
77	Asymmetric Multifunctional Heterogeneous Membranes for pH―and Temperature ooperative Smart Ion Transport Modulation. Advanced Materials, 2016, 28, 9613-9619.	11.1	83
78	Lightâ€Controlled Ion Transport through Biomimetic DNAâ€Based Channels. Angewandte Chemie - International Edition, 2016, 55, 15637-15641.	7.2	104
79	"Uphill―cation transport: A bioinspired photo-driven ion pump. Science Advances, 2016, 2, e1600689.	4.7	71
80	Construction and application of photoresponsive smart nanochannels. Journal of Photochemistry and Photobiology C: Photochemistry Reviews, 2016, 26, 31-47.	5.6	52
81	A Bioinspired Switchable and Tunable Carbonateâ€Activated Nanofluidic Diode Based on a Single Nanochannel. Angewandte Chemie - International Edition, 2015, 54, 13664-13668.	7.2	85
82	Fabrication of Nanochannels. Materials, 2015, 8, 6277-6308.	1.3	24
83	Photoelectron Spectroscopy and Density Functional Calculations of VGe <sub><i>n</i></sub> <sup>–</sup> ( <i>n</i> = 3–12) Clusters. Journal of Physical Chemistry C, 2015, 119, 11048-11055.	1.5	63
84	DNAzyme tunable lead( <scp>ii</scp> ) gating based on ion-track etched conical nanochannels. Chemical Communications, 2015, 51, 5979-5981.	2.2	50
85	Engineered Asymmetric Heterogeneous Membrane: A Concentration-Gradient-Driven Energy Harvesting Device. Journal of the American Chemical Society, 2015, 137, 14765-14772.	6.6	299
86	Probing the early stages of salt nucleation—Experimental and theoretical investigations of sodium/potassium thiocyanate cluster anions. Journal of Chemical Physics, 2015, 142, 024313.	1.2	10
87	Engineered Ionic Gates for Ion Conduction Based on Sodium and Potassium Activated Nanochannels. Journal of the American Chemical Society, 2015, 137, 11976-11983.	6.6	184
88	Smallest fullerene-like silicon cage stabilized by a V2 unit. Journal of Chemical Physics, 2014, 140, 024308.	1.2	47
89	Structural and Magnetic Properties of CoGe <sub><i>n</i></sub> <sup>â^'</sup> ( <i>n</i> =2–11) Clusters: Photoelectron Spectroscopy and Density Functional Calculations. ChemPhysChem, 2014, 15, 3987-3993.	1.0	57
90	Identification of hyperhalogens in Ag <sub>n</sub> (BO <sub>2</sub> ) <sub>m</sub> (n = 1–3, m = 1–2) clusters: anion photoelectron spectroscopy and density functional calculations. Physical Chemistry Chemical Physics, 2014, 16, 26067-26074.	1.3	12

#	Article	IF	CITATIONS
91	Photoelectron spectroscopy of lithium and gold alloyed boron oxide clusters: charge transfer complexes, covalent gold, hyperhalogen, and dual three-center four-electron hyperbonds. Physical Chemistry Chemical Physics, 2014, 16, 5129.	1.3	22
92	Structural and bonding properties of small TiGe <sub>n</sub> <sup>â^'</sup> (n = 2–6) clusters: photoelectron spectroscopy and density functional calculations. RSC Advances, 2014, 4, 25963-25968.	1.7	27
93	Examining the Amine Functionalization in Dicarboxylates: Photoelectron Spectroscopy and Theoretical Studies of Aspartate and Glutamate. Journal of Physical Chemistry A, 2014, 118, 5256-5262.	1.1	5
94	Vibrationally Resolved Photoelectron Spectroscopy of the Model GFP Chromophore Anion Revealing the Photoexcited S <sub>1</sub> State Being Both Vertically and Adiabatically Bound against the Photodetached D <sub>0</sub> Continuum. Journal of Physical Chemistry Letters, 2014, 5, 2155-2159.	2.1	34
95	Interaction of TiO+ with water: infrared photodissociation spectroscopy and density functional calculations. Physical Chemistry Chemical Physics, 2013, 15, 17126.	1.3	18
96	Investigation of (m=2–5,n=2–3) clusters using photoelectron spectroscopy and density functional calculations. Chemical Physics Letters, 2013, 564, 6-10.	1.2	2
97	Photoelectron spectroscopy and density functional calculations of AgSinâ^' (n = 3–12) clusters. Journal of Chemical Physics, 2013, 138, 244312.	1.2	26
98	Anomalous Property of Ag(BO <sub>2</sub> ) <sub>2</sub> Hyperhalogen: Does Spin–Orbit Coupling Matter?. ChemPhysChem, 2013, 14, 3303-3308.	1.0	15
99	Structures and magnetic properties of CrSinâ^' (n = 3–12) clusters: Photoelectron spectroscopy and density functional calculations. Journal of Chemical Physics, 2012, 137, 064307.	1.2	70
100	Microscopic solvation of NaBO2 in water: anion photoelectron spectroscopy and ab initio calculations. Physical Chemistry Chemical Physics, 2011, 13, 15865.	1.3	23
101	Anion Photoelectron Spectroscopy and Density Functional Study of Small Aluminumâ^'Vanadium Oxide Clusters. Journal of Physical Chemistry A, 2011, 115, 13-18.	1.1	22